(34%) responded significantly better to closer stimuli but were unaffected by the amplitude of the stimulus; 15 (34%) responded significantly better to higher-amplitude stimuli but were unaffected by the distance to the stimulus; and 11 (25%) responded significantly better to closer stimuli and, independently, to higher-amplitude stimuli. Amplitude is one of many possible cues that humans use to determine the distance to an auditory event[17]. Therefore, we suggest that the amplitude-sensitive neurons described here use this particular cue to code distance. These neurons will tend to respond to nearby stimuli because they respond better to higher-amplitude sounds. However, more than half of the neurons (59%) code distance by means of some other cue or combination of cues, such that they respond to nearby stimuli independently of the amplitude. Reverberation of the sound from the walls of the room may be important[18]. Another possible set of cues for distance involves familiarity with the sound source[19]. However, the first neuron tested in monkey 2 was significantly dependent on distance even though the monkey had never heard the stimulus before. Another possible cue is the difference in amplitude between the two ears; a very large difference implies a sound source close to one ear. However, the neurons were sensitive to distance even when the stimulus was presented on the midline, that is, when the amplitude was equal in both ears. Finally, the calculation of distance near the head may depend on the highly complex distorting effect of the head and pinnae on the sound spectrum[1]. This last effect would be especially pronounced at such close distances as 10 cm. A full analysis of the relative influence of these different cues will require further experiments.

The cortical pathways for auditory spatial processing are not well understood. Perhaps distance information is calculated in a different brain area and then relayed to the trimodal neurons in PMv. Recently, we studied neurons in a portion of parietal area 7b[20], in the upper bank of the later sulcus, and found similar trimodal, tactile–visual–auditory neurons (M.S.A.G. and C.G.G., manuscript in preparation). Area 7b projects to PMv[21,22], but whether the trimodal region of 7b projects to the trimodal region of PMv has not yet been determined.

Previous experiments showed that multimodal neurons in PMv encode the locations of nearby objects, within about reaching distance, through touch, vision, and even visual memory[11–16]. Our results show that PMv neurons also represent nearby auditory space. Because a high proportion of PMv neurons respond during movements of the head, mouth, arms and hands, the purpose of this multimodal map of space may be to guide movements towards and around the objects that surround the body[23,24]. □

Methods

Two adult *M. fascicularis* were trained to sit in a primate chair; they did not perform any task. (For details of the experimental procedures, see ref. 16.) During daily recording sessions, a microdrive was used to lower an electrode into PMv. Once a neuron was isolated, it was tested for somatosensory, visual and auditory responses. Somatosensory receptive fields were plotted by manipulating the joints and stroking the skin. Visual receptive fields were plotted with objects presented on a wand. Auditory stimuli included tones, clicks, claps, jingling keys and other sounds. Controlled tests were done using white noise (20–22,000 Hz) presented over Cambridge Soundworks 3-inch (76.2 mm) speakers mounted in a circular array around the monkey's head at ear level. The angular position and distance of the speakers to the head was adjustable. The sound pressure level of the stimuli was measured at the monkey's head using a Radio Shack sound level meter, repeatedly calibrated with a 0.25-inch (6.35 mm) Bruel and Kjaer microphone. Neurons were tested either with the speaker behind the head, or in the dark, so that the monkey could not see the distance to the sound source. Eye position was not controlled during the presentation of auditory stimuli. Some PMv neurons are influenced by eye position[14,16,25]. However, the short latency of the auditory response eliminates the possibility that it was caused by a change in eye position elicited by the presentation of the stimulus. In addition, there are no reports of transient bursts of activity in PMv associated with eye movement, whereas most of the auditory responses in PMv were transient, short-latency bursts (Fig. 1b).

Received 29 September; accepted 23 November 1998.

1. Blauert, J. *Spatial Hearing: The Psychophysics of Human Sound Localization* (transl. Allen, J. S.) (MIT Press, Cambridge, Massachusetts, 1997).
2. Clifton, R. K., Rochat, P., Robin, D. J. & Berthier, N. E. Multimodal perception in the control of infant reaching. *J. Exp. Psychol. Hum. Percept. Perform.* **20,** 876–886 (1994).
3. Coleman, P. D. An analysis of cues to auditory depth perception in free space. *Psychol. Bull.* **60,** 302–315 (1963).
4. Coleman, P. D. Dual role of frequency spectrum in determination of auditory distance. *J. Acoust. Soc. Am.* **44,** 631–632 (1968).
5. Edwards, A. A. Accuracy of auditory depth perception. *J. Gen. Psychol.* **52,** 327–329 (1955).
6. Gamble, E. A. Intensity as a criterion in estimating the distance of sounds. *Psychol. Rev.* **16,** 416–426 (1909).
7. Gardner, M. B. Distance estimation of 0° or apparent 0°-oriented speech signals in anechoic space. *J. Acoust. Soc. Am.* **45,** 47–53 (1969).
8. Mershon, D. H. & Bowers, J. N. Absolute and relative cues for the auditory perception of egocentric distance. *Perception* **8,** 311–322 (1979).
9. von Bekesy, G. *Experiments in Hearing* (McGraw-Hill, New York, 1960).
10. Suga, N. & O'Neill, W. E. Neural axis representing target range in the auditory cortex of the mustache bat. *Science* **206,** 351–353 (1979).
11. Gentilucci, M. *et al.* Functional organization of inferior area 6 in the macaque monkey. I. Somatotopy and the control of proximal movements. *Exp. Brain. Res.* **71,** 475–490 (1988).
12. Fogassi, L. *et al.* Coding of peripersonal space in inferior premotor cortex (area F4). *J. Neurophysiol.* **76,** 141–157 (1996).
13. Graziano, M. S. A., Yap, G. S. & Gross, C. G. Coding of visual space by pre-motor neurons. *Science* **266,** 1054–1057 (1994).
14. Graziano, M. S. A., Hu, X. & Gross, C. G. Coding the locations of objects in the dark. *Science* **277,** 239–241 (1997).
15. Rizzolatti, G. *et al.* Afferent properties of periarcuate neurons in macaque monkeys. II. Visual responses. *Behav. Brain Res.* **2,** 147–163 (1981).
16. Graziano, M. S. A., Hu, X. & Gross, C. G. Visuo-spatial properties of ventral premotor cortex. *J. Neurophysiol.* **77,** 2268–2292 (1997).
17. Ashmead, D. H., LeRoy, D. & Odom, R. D. Perception of the relative distances of nearby sound sources. *Percept. Psychophys.* **47,** 326–331 (1990).
18. Mershon, D. H. & King, L. E. Intensity and reverberation as factors in the auditory perception of egocentric distance. *Percept. Psychophys.* **18,** 409–415 (1975).
19. Coleman, P. D. Failure to localize the source distance of an unfamiliar sound. *J. Acoust. Soc. Am.* **34,** 345–346 (1962).
20. Graziano, M. S. A., Fernandez, T. & Gross, C. G. A comparison of bimodal, visual-tactile neurons in parietal area 7b and ventral premotor cortex of the monkey brain. *Neurosci. Abs.* **22,** 398 (1996).
21. Cavada, C. & Goldman-Rakic, P. S. Posterior parietal cortex in rhesus monkey: II: Evidence for segregated corticocortical networks linking sensory and limbic areas with the frontal lobe. *J. Comp. Neurol.* **287,** 422–445 (1989).
22. Matelli, M., Camarda, R., Glickstein, M. & Rizzolatti, G. Afferent and efferent projections of the inferior area 6 in the macaque monkey. *J. Comp. Neurol.* **255,** 281–298 (1986).
23. Graziano, M. S. A. & Gross, C. G. Spatial maps for the control of movement. *Curr. Opin. Neurobiol.* **8,** 195–201 (1998).
24. Rizzolatti, G., Fadiga, L., Fogassi, L. & Gallese, V. The space around us. *Science* **277,** 190–191 (1997).
25. Boussaoud, D., Barth, T. M. & Wise, S. P. Effects of gaze on apparent visual responses of frontal cortex neurons. *Exp. Brain Res.* **93,** 423–434 (1993).
26. Cohen, J. & P. Cohen, P. *Applied Multiple Regression/Correlation Analysis for the Behavioral Sciences* (Lawrence Earlbaum Associates, Hillsdale, New Jersey, 1983).

Acknowledgements. We thank E. Olson, X. Hu, S. Alisharan, M. E. Wheeler and V. Gomez for their help during the experiment.

Correspondence and requests for materials should be addressed to M.S.A.G. (e-mail: graziano@princeton.edu).

Perception's shadow: long-distance synchronization of human brain activity

Eugenio Rodriguez, Nathalie George, Jean-Philippe Lachaux, Jacques Martinerie, Bernard Renault & Francisco J. Varela

Laboratoire de Neurosciences Cognitives et Imagerie Cérébrale (LENA), CNRS UPR 640, Hôpital de la Salpétrière, 47 Boulevard de l'Hôpital, 75651 Paris Cedex 13, France

Transient periods of synchronization of oscillating neuronal discharges in the frequency range 30–80 Hz (gamma oscillations) have been proposed to act as an integrative mechanism that may bring a widely distributed set of neurons together into a coherent ensemble that underlies a cognitive act[1–4]. Results of several experiments in animals provide support for this idea (see, for example, refs 4–10). In humans, gamma oscillations have been

described both on the scalp[11–16] (measured by electroencephalography and magnetoencephalography) and in intracortical recordings[17], but no direct participation of synchrony in a cognitive task has been demonstrated so far. Here we record electrical brain activity from subjects who are viewing ambiguous visual stimuli (perceived either as faces or as meaningless shapes). We show for the first time, to our knowledge, that only face perception induces a long-distance pattern of synchronization, corresponding to the moment of perception itself and to the ensuing motor response. A period of strong desynchronization marks the transition between the moment of perception and the motor response. We suggest that this desynchronization reflects a process of active uncoupling of the underlying neural ensembles that is necessary to proceed from one cognitive state to another[3].

Ten subjects were shown 'Mooney' faces (Fig. 1a, b), which are easily categorized as faces when presented in upright orientation, but usually seen as meaningless black and white shapes when presented upside-down[18,19]. Subjects were asked to report as quickly as possible whether they had seen a face or not by pressing on one of two different keys. On average, 79 ± 2% of upright presentations were perceived as faces. Conversely, 76 ± 2% of upside-down presentations were reported as meaningless. We analysed only the cases of upright presentations that were perceived as faces and inverted presentations that were perceived as meaningless, referred to here as the 'perception' and 'no-perception' conditions. The electroencephalogram (EEG) was recorded through 30 electrodes, and a precise time–frequency analysis was carried out up to 100 Hz.

We first computed the pseudo Wigner–Ville time–frequency transforms[20] of single trials and averaged these transforms over all trials. This procedure is best adapted to detect the so-called 'induced' gamma response, which is triggered by, but not phase-locked to, stimulus onset[15] ('phase-locking' is synchronization of oscillations). We obtained two induced gamma-activity peaks (Fig. 1c, d). The first induced response, lying at 36 ± 3 Hz for both conditions, peaked at ~230 ms after stimulus onset, was significantly larger for the perception condition (Wilcoxon $T = 5$, $Z = 2.29$, $P < 0.05$) and has been consistently described as the correlate of the perceptual process itself[11–17]. Similar conclusions are reached by studies of evoked potential[21]. In contrast, the second induced gamma peak has not been reported so far. It peaked at ~800 ms with a maximum frequency of 40 ± 5 Hz, following the subject's reaction time closely, and was slightly (but not significantly) stronger in the no-perception than in the perception condition. The latency of this peak indicates the possible involvement of post-perceptual processes.

We then studied phase synchrony, the main focus of our work. We

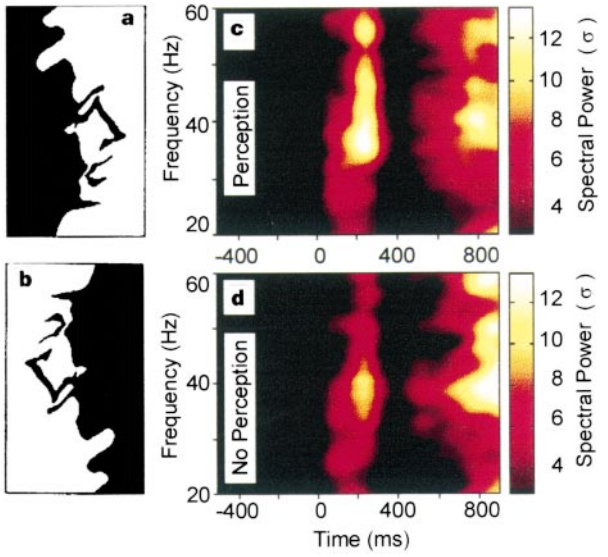

Figure 1 Stimuli and emission time–frequency charts. **a**, **b**, Examples of 'Mooney' faces, high-contrast pictures of a human face. These pictures are easily recognized as human faces when seen upright (**a**), but are difficult to recognize when inverted (**b**). **c**, **d**, Spectral power following stimulation. A time–frequency transform was computed in each trial and then summed over all trials, subjects and electrodes. The chart retains mainly the induced component of the gamma response. Both charts exhibit two periods of increased gamma-power emission (between 20 and 60 Hz). Power peaks at ~230 ms after stimulus onset, and between 33 and 39 Hz. The perception condition elicits a significantly stronger gamma response than the no-perception condition (Wilcoxon $T = 5$, $Z = 2.29$, $P < 0.05$). The second peak lies at ~800 ms and 40 ± 5 Hz; it follows after the reaction time (645 ± 20 ms for perception; 766 ± 22 ms for no-perception) and no significant differences between conditions are found. The colour scale is indicated in standard deviations, calculated from the 500-ms baseline. We are summarizing our results here, but 7 out of 10 individual results were also significant.

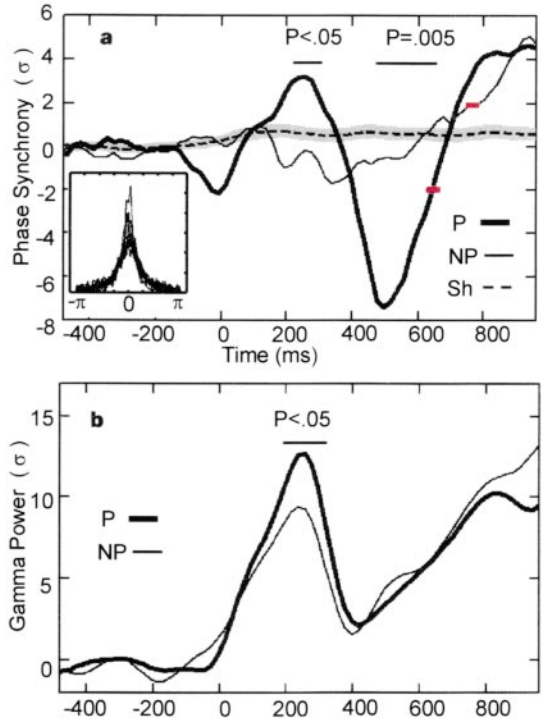

Figure 2 Time courses of phase synchrony and gamma activity. Results shown are averages over trials, electrodes, and subjects. Values are in standard deviations from the 500-ms baseline. Thick line, face-perception condition (P); thin line, no-perception condition (NP); dashed line, synchrony computed on shuffled data (Sh); the grey strip indicates dispersion of these data ±3 standard errors; horizontal red lines indicate ± standard error of reaction time. **a**, Phase synchrony for the P and NP conditions. NP synchrony remains stable and near the shuffling average until 700 ms. Phase synchrony for the P condition increases at 230 ms ($P < 0.05$), decreases sharply at 500 ms ($P = 0.005$; absolute value of 0.3), and ends with a second increase. Synchrony is measured with a 250-ms long wavelet; a commensurable spread of synchrony follows, thus explaining results that seem to begin before stimulation onset. Inset, phase-lag distributions for ten increasingly distant synchronic electrode pairs; for all distributions $\mu = 0$ and $\sigma \approx 40°$. **b**, Gamma-power activity in the 34–40 Hz band. In contrast to phase synchrony, and despite the presence of a significant difference in synchrony at 250 ms, both conditions follow a similar time course of gamma-band activity.

introduced an effective method[22] with which to directly measure phase-locking; this method is based on wavelet filtering followed by trial-by-trial comparison of phase differences, and overcomes the shortcomings of other techniques used previously[5,23,24]. Electrical activity was taken to be synchronous if phase lag between two electrodes remained constant throughout all the trials.

The main results obtained from our studies of phase synchrony are summarized in Fig. 2a and compared to gamma activity in Fig. 2b. Phase synchrony differed markedly between the perception and no-perception conditions (Fig. 2a). Only the perception condition elicited a three-part temporal pattern spanning the entire duration of the task, from stimulus presentation to motor response. First, a significant increase in synchrony for the perception relative to the no-perception condition occurred at ~200–260 ms after stimulus presentation (Wilcoxon $T = 8$, $Z = 1.99$, $P < 0.05$); the temporal coincidence of this increase in synchrony with the first gamma response indicates a functional involvement of this increase in perception itself. It was followed by a marked decrease in synchrony, or desynchronization, centred at 500 ms (Wilcoxon $T = 0$, $Z = 2.8$, $P < 0.005$). A final increase in synchrony was present for both conditions at about the reaction time (645 ± 20 ms of standard error for perception; 766 ± 22 ms for non-perception). Furthermore, synchronic electrodes had zero-centred phase-lag distributions, regardless of interelectrode distance (Fig. 2, inset). In contrast to synchrony, gamma activity for both the perception and the no-perception conditions did not yield qualitative differences, but only an amplitude difference at 230 ms (Fig. 2b).

The stage of sharp decrease of phase synchrony has not been described before, to our knowledge, but it appears as a very significant effect in our results ($P = 0.005$). Given the method used for computing synchrony, this decrease cannot be interpreted as a return to the baseline level of synchrony (see Methods). We suggest that it reflects a process of active desynchronization. This result provides the first direct support for the previous proposal[3] that a transition between two distinct cognitive acts (such as face perception and motor response) should be punctuated by a transient stage of undoing the preceding synchrony and allowing for the emergence of a new ensemble, through cellular mechanisms that remain to be established.

To validate our results, we compared them with synchronies computed in shuffled trials, a technique used widely in single-cell studies[4,9,10]. Shuffling is done by randomizing the order of trials and calculating synchronies between events that were not recorded at the same time. This allows an estimation of the magnitude of the background random fluctuations for the values of synchrony as measured here. The average of shuffled synchronies varied little over the entire observation window and showed limited variance, in contrast to both of our experimental conditions (Fig. 2a). Thus our results do not represent random phase coincidences present in scalp recordings.

Detailed spatiotemporal information is provided by the regional distribution of gamma activity and phase synchrony over the scalp (Fig. 3). The pattern of gamma activity was spatially homogeneous and was similar between the perception and no-perception conditions over time, differing only in amplitude. In contrast, the pattern of synchrony was spatially unhomogeneous and differed over time between conditions. Compared with the no-perception condition, which showed few synchronous patterns, the perception condition exhibited a sequence of localized spatial patterns that evolved over time (Fig. 3). Synchrony first increased in the area between the left parieto-occipital and frontotemporal regions. Desynchronization was then observed between the parietal and occipitotemporal areas bilaterally. Parietal regions are involved in visual perception[25,26] and episodic memory[27]. Interactions between these regions and occipitotemporal regions, in particular the fusiform gyrus, have been linked to perceptual learning of degraded Mooney-like faces[25]. We propose that phase interactions between parietal and occipitotemporal regions are essential in the large-scale integration that is needed for the perception of upright Mooneys as faces. The second synchrony increase, which is probably linked to motor response, was predominant between the right temporal and central regions. Only during this second period of increase were there slight similarities between the perception and no-perception conditions, because the subject responded in both cases.

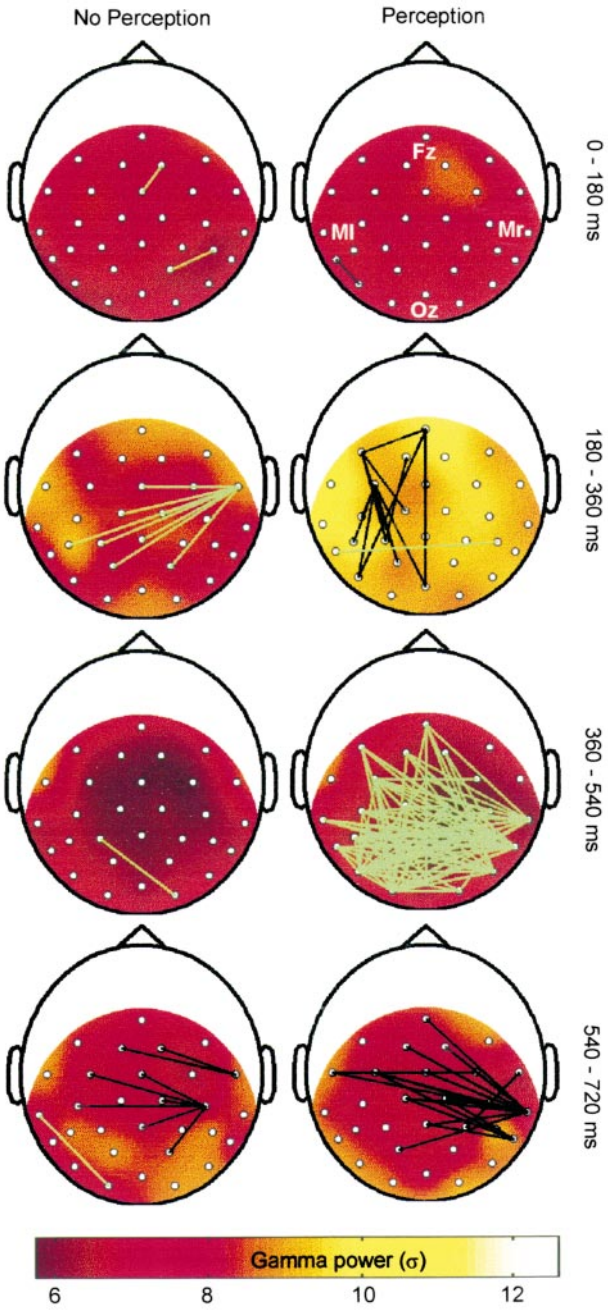

Figure 3 The shadow of a perception. Average scalp distribution of gamma activity and phase synchrony. Colour coding indicates gamma power (averaged in a 34–40-Hz frequency range) over an electrode and during a 180-ms time window, from stimulation onset (0 ms) to motor response (720 ms). Gamma activity is spatially homogeneous and similar between conditions over time. In contrast, phase synchrony is markedly regional and differs between conditions. Synchrony between electrode pairs is indicated by lines, which are drawn only if the synchrony value is beyond the distribution of shuffled data sets ($P < 0.01$; see Methods). Black and green lines correspond to a significant increase or decrease in synchrony, respectively.

The biological significance of phase synchrony computed from scalp EEGs has been doubted because it is difficult to rule out the occurrence of spurious synchronization resulting from volume conduction[23]. However, such spurious synchronization cannot account for our results. Volume conduction induces a pattern of synchronization that decays rapidly as the separation between electrodes increases beyond 2 cm on the surface of the cortex[23]. In contrast, we found that synchrony can be established between recording sites situated far away from each other on the head surface; only 7% of the synchronies reported here were between neighbouring recording sites. It is also conceivable that distant synchronization could result from a powerful deep source that diffuses widely over the scalp. But if this were the case, the phase-synchrony pattern should coincide with gamma activity, the electrodes with higher emission being the most synchronous ones. Our results do not show this (Fig. 3). Finally, the desynchronizing periods found here are impossible to explain by volume conduction. If synchrony effects were just a reflection of gamma activity then desynchronization should be associated with periods of low gamma activity. Our results show the opposite effect: desynchronization co-existed with periods of above-average gamma activity. Furthermore, the same gamma level led to strong desynchronization in the perception condition but had no effect on the no-perception condition (Fig. 2). Finally, the zero-centred phase-lag distribution found here also suggests that the measured synchronies did not have an artefactual origin.

The finding of gamma oscillations has often been taken, erroneously, as an indication of synchrony. Indeed, changes in gamma-band spectral content cannot be conflated with the phase synchrony between pairs of electrodes at which such gamma activity occurs. Only synchrony measures bear directly on the possible role of gamma activity in cognition, as synchrony provides direct information about electrode pairs and their regional location, which power emission alone cannot provide. To our knowledge, our results are the first to support the theory that phase synchrony is directly involved in human cognition. The long-range character of the phase synchrony indicates that gamma-phase synchrony (and desynchrony) may be viewed as a mechanism that subserves large-scale cognitive integration[2,3,5,8], and not just local visual-feature binding. Finally, we stress that the detection of phase synchrony/desynchrony over the scalp amounts to a dynamic brain mapping that is essential for the study of the neural basis of cognitive tasks. □

Methods

Protocol and recordings. Experimental design[19] and data analysis[22] have been described in detail elsewhere. In brief, Mooney faces were presented randomly for 200 ms in upright or inverted position, in a total of 320 trials. Ten subjects (20–30 years old; seven females) gave their response by pressing buttons situated under their right and left index fingers. EEGs were recorded by 30 electrodes at standard 10–20 positions, to which we added a lower row (M1, M2, P9, P10, PO9, PO10, O9, and O10). Sampling was taken at 500 Hz.

Time–frequency analysis. After automatic correction of eye-movement artefact trials, signals were high-pass-filtered at 15 Hz and time–frequency-analysed using the pseudo Wigner–Ville transformation[17,20]. Resulting time–frequency maps were normalized and averaged through trials, electrodes and subjects.

Phase-synchrony detection. Previous methods for measuring phase synchrony between electrode pairs have included spectral coherence[5,23], which mixes energy and phase information, and detection of maximal values after filtering[24], which is inaccurate and slow when large data sets are involved. In the method introduced here, for each subject phase synchrony was computed only for the frequency f_0 of his/her maximal gamma activity (varying from 35 to 45 Hz, depending on the subject). Phase was measured from narrow-band-filtered signals ($f_0 \pm 3$ Hz) by convolution with a complex Gabor wavelet designed for f_0. An instantaneous phase value, $\varphi_i(f_0, t, k)$, which is a complex number of unit magnitude, was thus obtained for one electrode, i, a chosen frequency, f_0, at time bin indexed by t, and trial k. For each electrode pair, i and j, and time t, and for all of the $k = 1, \ldots, N$ trials, a global phase-locking value $\varphi_{ij}(f_0, t)$ is computed as:

$$\varphi_{ij}(f,t) = \frac{\left|\sum_k \varphi_i - \varphi_j\right|}{N}$$

φ_{ij} is a real value bounded between 1 (if phase difference is constant) and 0 (if phase difference is random).

Normalization. To calculate synchrony values comparable between near (<2 cm) and distant electrode pairs, we carried out a normalization procedure so that the $\varphi_{ij}(f, t)$ values were compared with the 500-ms baseline preceding the stimulus. Given φ_{ij}, let μ_{ij} and σ_{ij} be the mean and standard deviation computed from a 500-ms prestimulus baseline; the normalized phase-locking values are then computed as $\bar{\varphi}_{ij} = (\varphi_{ij} - \mu_{ij})/\sigma_{ij}$. The same normalization procedure is applied to time–frequency matrices on a frequency-by-frequency basis.

Topographical synchrony. To display the lines indicating synchrony over individual pairs of electrodes (Fig. 3) we used the following statistical procedure. Let W_k be a 180-ms time window between stimulus arrival and motor response, and let $\varphi_{ij}(W_k)$ be the average phase synchrony between electrodes i and j over the entire time window, W_k. To enhance time changes, we compared W_k with the previous time window, W_{k-1}, and defined the phase-locking value between pairs finally as $\Delta\varphi_{ij}(W_k) = \varphi_{ij}(W_k) - \varphi_{ij}(W_{k-1})$. For each $\Delta\varphi_{ij}(W_k)$, 200 values were analogously computed on shuffled data $\Delta\varphi^s_{ij}(W_k)$. A $\Delta\varphi_{ij}$ value is retained as statistically significant only if greater than (or lesser than) any of the 200 shuffled values $\Delta\varphi^s_{ij}$, thus corresponding to a two-tailed probability value of $P = 0.01$.

Received 7 October; accepted 23 December 1998.

1. Freeman, W. J. *Mass Action in the Nervous System* (Academic, New York, 1975).
2. Damasio, A. R. Synchronous activation in multiple cortical regions: a mechanism for recall. *Semin. Neurosci.* **2,** 287–297 (1990).
3. Varela, F. J. Resonant cell assemblies: a new approach to cognitive function and neuronal synchrony. *Biol. Res.* **28,** 81–95 (1995).
4. Singer, W. & Gray, C. M. Visual feature integration and the temporal correlation hypothesis. *Annu. Rev. Neurosci.* **18,** 555–586 (1995).
5. Bressler, S. L., Coppola, R. & Nakamura, R. Episodic multiregional cortical coherence at multiple frequencies during visual task performance. *Nature* **366,** 153–156 (1993).
6. Gray, C. M., König, P., Engel, A. K. & Singer, W. Oscillatory responses in cat visual cortex exhibit inter-columnar synchronization which reflects global stimulus properties. *Nature* **338,** 334–337 (1989).
7. Vaadia, E. *et al.* Dynamics of neuronal interaction in the monkey cortex in relation to behavioral events. *Nature* **373,** 515–518 (1995).
8. Roelfsema, P. R., Engel, A. K., König, P. & Singer, W. Visuomotor integration is associated with the zero time-lag synchronization among cortical areas. *Nature* **385,** 157–161 (1997).
9. Neuenschwander, S., Engel, A., König, P., Singer, W. & Varela, F. Synchronization of neuronal responses in the optic tectum of awake pigeons. *Vis. Neurosci.* **13,** 575–584 (1996).
10. Kreiter, A. K. & Singer, W. Stimulus-dependent synchronization of neuronal responses in the visual cortex of the awake macaque monkey. *J. Neurosci.* **16,** 2381–2396 (1996).
11. Llinas, R. & Ribary, U. Coherent 40 Hz oscillation characterizes dream state in humans. *Proc. Natl Acad. Sci. USA* **90,** 2078–2081 (1993).
12. Tiitinen, H. *et al.* Selective attention enhances the auditory 40-Hz transient response in humans. *Nature* **364,** 59–60 (1993).
13. Desmedt, J. E. & Tomberg, C. Transient phase-locking of 40 Hz electrical oscillations in prefrontal parietal cortex reflects the process of conscious somatic perception. *Neurosci. Lett.* **168,** 126–129 (1994).
14. Joliot, M., Ribary, U. & Llinas, R. Human oscillatory brain activity near 40 Hz coexists with cognitive temporal binding. *Proc. Natl Acad. Sci. USA* **91,** 11748–11751 (1994).
15. Pantev, C. Evoked and induced gamma band activity of the human cortex. *Brain Topogr.* **7,** 321–330 (1995).
16. Tallon-Baudry, C., Bertrand, O., Delpuech, C. & Pernier, J. Oscillatory gamma band (30–70 Hz) activity induced by a visual search task in human. *J. Neurosci.* **17,** 722–734 (1997).
17. Lachaux, J. P. *et al.* Gamma band activity in human intracortical recordings triggered by cognitive tasks. *Eur. J. Neurosci.* (submitted).
18. Mooney, C. M. Age in the development of closure ability in children. *Can. J. Psychol.* **11,** 219–226 (1957).
19. George, N., Jemel, B., Fiori, N. & Renault, B. Face and shape repetition effects in humans: a spatio-temporal ERP study. *NeuroReport* **8,** 1417–1423 (1997).
20. Mecklenbräuker, W. F. G. (ed.) *The Wigner Distribution—Theory and Applications in Signal Processing* (Elsevier, Amsterdam, 1993).
21. Jeffreys, D. A. Evoked potentials studies of face and object processing. *Vis. Cogn.* **3,** 1–38 (1996).
22. Lachaux, J. P., Rodriguez, E., Müller-Gerking, J., Martinerie, J. & Varela, F. J. Measuring phase-synchrony in brain signals. *Hum. Brain Mapp.* (submitted).
23. Menon, V. *et al.* Spatio-temporal correlations in human gamma band electrocorticograms. *Electroencephalogr. Clin. Neurophysiol.* **98,** 89–102 (1996).
24. Yordanova, J., Kolev, V. & Demiralp, T. The phase-locking of auditory gamma band responses in humans is sensitive to task processing. *NeuroReport* **8,** 3999–4004 (1997).
25. Dolan, R. J. *et al.* How the brain learns to see objects and faces in an impoverished context. *Nature* **389,** 596–599 (1997).
26. Friedman-Hill, S. R., Robertson, L. C. & Treisman, A. Parietal contributions to visual feature binding: evidence from a patient with bilateral lesions. *Science* **269,** 853–855 (1995).
27. Shallice, T. *et al.* Brain regions associated with acquisition and retrieval of verbal episodic memory. *Nature* **368,** 633–635 (1994).

Acknowledgements. We thank Y. Okada for suggestions on the manuscript. This work was supported by grants from MIDEPLAN (Chile), DRET (France), and the Human Science Frontier.

Correspondence and requests for materials should be addressed to F.J.V. (e-mail: fv@ccr.jussieu.fr).